suggesting down-regulation of DNA replication and providing evidence for a role of human Orc6 in DNA replication. BrdU incorporation studies revealed 60 to 70% cells positive for BrdU after 60 hours of transfection, and decreased to 20 to 30% cells after 108 hours (Fig. 5A). In the majority of multinucleate cells, one or two nuclei showed much lower than normal BrdU staining and the remaining nuclei had no BrdU incorporation over a 24-hour period (Fig. 5B). Some cells transfected with Orc6 siRNA duplexes showed an overall intensity of BrdU staining considerably lower than that observed in control cells (see figs. S5 and S6), suggesting infrequent replication origin-firing. Because the origins of DNA replication are redundant, it is likely that most of the Orc6 had to be depleted to reveal a complete defect in DNA replication. BrdU incorporation followed by colcemid-induced metaphase spreads following 108 hours of Orc6 siRNA showed incomplete and lower levels of BrdU incorporation during a 24-hour label (Fig. 5C) (fig. S7). However, the control cells (GI3) showed complete staining of duplicated chromosomes. The punctate incorporation of BrdU suggests that fewer origins fire, resulting in a slower S phase. Similarly, *Drosophila* larvae homozygous for Orc2 and Orc5 mutants progressed slowly through S phase and showed vastly reduced BrdU incorporation; these defects may have been caused by fewer active origins (*24*).

In human cells, Orc6 functions in multiple aspects of the cell division cycle, including DNA replication, chromosome segregation, and cytokinesis. It may be that Orc6 participates independently in the mechanics of DNA replication, centromere function, and cytokinesis. Alternatively, a significant defect in DNA replication caused by silencing of Orc6 might trigger aberrant mitosis (or other downstream effects) by interfering with centrosome duplication (*25*). Although this scenario could explain the spindle defects and polyploidy, it would not explain the cytokinesis defects in cells lacking Orc6. A reduction in DNA replication after Orc2 siRNA treatment did not yield similar phenotypes. Also, the Orc6 siRNA phenotypes are consistent with Orc6 distribution to the kinetochores and midbody. A third possibility is consistent with the Orc6 localization pattern during the cell cycle: Orc6 could be essential for inducing or signaling to multiple cell cycle checkpoints that coordinate the many processes of the cell division cycle (*26*). In this model, chromosome duplication, segregation, and cytokinesis would be coordinated by a common participant. A protein such as Orc6 could cycle from origins of DNA replication to centromeres and the cytokinesis apparatus to ensure the correct order and coordination of events.

References and Notes

1. S. Waga, B. Stillman, *Annu. Rev. Biochem.* **67**, 721 (1998).
2. S. P. Bell, *Genes Dev.* **16**, 659 (2002).
3. ———, B. Stillman, *Nature* **357**, 128 (1992).
4. T. J. Kelly, G. W. Brown, *Annu. Rev. Biochem.* **69**, 829 (2000).
5. I. Chesnokov, M. Gossen, D. Remus, M. Botchan, *Genes Dev* **13**, 1289 (1999).
6. I. Chesnokov, D. Remus, M. Botchan, *Proc. Natl. Acad. Sci. U.S.A.* **98**, 11997 (2001).
7. J. Mendez *et al.*, *Mol. Cell* **9**, 481 (2002).
8. A. A. Van Hooser, M. A. Mancini, C. D. Allis, K. F. Sullivan, B. R. Brinkley, *FASEB J.* **13** (suppl. 2), S216 (1999).
9. S. G. Prasanth, B. Stillman, unpublished data.
10. D. A. Skoufias, P. R. Andreassen, F. B. Lacroix, L. Wilson, R. L. Margolis, *Proc. Natl. Acad. Sci. U.S.A.* **98**, 4492 (2001).
11. M. Glotzer, *Annu. Rev. Cell Dev. Biol.* **17**, 351 (2001).
12. S. G. Zeitlin, K. F. Sullivan, *Curr. Biol.* **11**, R514 (2001).
13. P. Fortugno *et al.*, *J. Cell Sci.* **115**, 575 (2002).
14. J. M. Mullins, J. R. McIntosh, *J. Cell Biol.* **94**, 654 (1982).
15. W. C. Earnshaw, R. L. Bernat, *Chromosoma* **100**, 139 (1991).
16. D. G. Lee, S. P. Bell, *Mol. Cell. Biol.* **17**, 7159 (1997).
17. M. Weinreich, C. Liang, H. H. Chen, B. Stillman, *Proc. Natl. Acad. Sci. U.S.A.* **98**, 11211 (2001).
18. P. J. Gillespie, A. Li, J. J. Blow, *BioMed Central Biochem.* **2**, 15 (2001).
19. S. M. Elbashir *et al.*, *Nature* **411**, 494 (2001).
20. Orc6 siRNA oligos 6.13 (5′-AAUGGUAGCCACAUCCGGUGU-3′) and 6.17 (5′-AAGATTGGACAGCAGGUCGAC-3′) were obtained from Dharmacon Research Inc.
21. R. R. Adams, H. Maiato, W. C. Earnshaw, M. Carmena, *J. Cell Biol.* **153**, 865 (2001).
22. A. G. Uren *et al.*, *Curr. Biol.* **10**, 1319 (2000).
23. J. Harborth, S. M. Elbashir, K. Bechert, T. Tuschl, K. Weber, *J. Cell Sci.* **114**, 4557 (2001).
24. M. F. Pflumm, M. R. Botchan, *Development* **128**, 1697 (2001).
25. O. C. Sibon, A. Kelkar, W. Lemstra, W. E. Theurkauf, *Nature Cell Biol.* **2**, 90 (2000).
26. H. Murakami, P. Nurse, *Biochem. J.* **349**, 1 (2000).
27. S. A. Jablonski, G. K. Chan, C. A. Cooke, W. C. Earnshaw, T. J. Yen, *Chromosoma* **107**, 386 (1998).
28. We thank all members of the Stillman laboratory for stimulating discussions; H. Zou-Yang and S. Dike for anti-ORC antibodies; T. J. Yen, B. R. Brinkley, K. H. A. Choo, and F. McKeon for kinetochore antibodies; A. Krainer for SF2/ASF antibody; D. L. Spector and D. Helfman for suggestions; J. Mendez, A. Stenlund, and G. Hannon for reading the manuscript; and J. Duffy for artwork and photography. Supported by National Cancer Institute grant CA13106.

Supporting Online Material

www.sciencemag.org/cgi/content/full/297/5583/1026/DC1

Figs. S1 to S7

11 April 2002; accepted 22 May 2002

Impaired B and T Cell Antigen Receptor Signaling in p110δ PI 3-Kinase Mutant Mice

Klaus Okkenhaug,[1] Antonio Bilancio,[1]* Géraldine Farjot,[1]* Helen Priddle,[2]*† Sara Sancho,[3] Emma Peskett,[1] Wayne Pearce,[1] Stephen E. Meek,[2] Ashreena Salpekar,[1] Michael D. Waterfield,[1,4] Andrew J. H. Smith,[2] Bart Vanhaesebroeck[1,4]‡

Class IA phosphoinositide 3-kinases (PI3Ks) are a family of p85/p110 heterodimeric lipid kinases that generate second messenger signals downstream of tyrosine kinases, thereby controlling cell metabolism, growth, proliferation, differentiation, motility, and survival. Mammals express three class IA catalytic subunits: p110α, p110β, and p110δ. It is unclear to what extent these p110 isoforms have overlapping or distinct biological roles. Mice expressing a catalytically inactive form of p110δ (p110δ^{D910A}) were generated by gene targeting. Antigen receptor signaling in B and T cells was impaired and immune responses in vivo were attenuated in p110δ mutant mice. They also developed inflammatory bowel disease. These results reveal a selective role for p110δ in immunity.

There is increasing evidence for an important role for class IA PI3Ks in regulation of the immune system (*1–4*). Mice lacking the p85α regulatory subunit show impaired B cell development and activation but normal T cell activation, whereas T cell–restricted deletion of the gene for the phosphoinositide 3-phosphatase PTEN, a negative regulator of PI3K signaling, results in a lethal lymphoproliferative disease (*5–7*). To date, the specific role for each of the three class IA PI3K catalytic subunits in lymphocyte signaling has not been determined. p110δ is expressed predominantly in leukocytes (*8*, *9*), which indicates that it may play a unique role in immune signaling.

The study of class IA PI3Ks is complicated by the heterodimeric nature of these proteins,

[1]Ludwig Institute for Cancer Research, 91 Riding House Street, London W1W 7BS, UK. [2]Gene Targeting Laboratory, Center for Genome Research, University of Edinburgh, West Mains Road, Edinburgh, EH9 3JQ, UK. [3]Frimorfo, Rue du Musée 12, CH-1705 Fribourg, Switzerland. [4]Department of Biochemistry and Molecular Biology, University College London, Gower Street, London WC1E 6BT, UK.

*These authors contributed equally to this report.
†Present address: Roslin Institute, Roslin, Midlothian, EH25 9PS, UK.
‡To whom correspondence should be addressed. E-mail: bartvanh@ludwig.ucl.ac.uk

and altering the expression of one subunit can affect the expression of the others (*10*). In cells from p85α knockout mice, p85β expression was up-regulated, and expression of p110α, p110β, and p110δ was down-regulated (*5*, *6*, *11*). In contrast, p85α was overexpressed in p110α knockout embryos, which died after 9.5 days of gestation (*12*). In this study, p110δ was inactivated by point mutation instead of by deletion to prevent changes in the expression levels of the other PI3K catalytic and regulatory subunits (see fig. S1 for details of the targeting strategy). Homozygous mutant mice ($p110\delta^{D910A/D910A}$) were born at normal Mendelian ratios, were fertile, and did not show gross anatomical or behavioral abnormalities (*13*).

Expression of the mutated p110δ protein was equivalent to that of the wild-type (WT) protein, as was the expression of the other PI3K subunits (Fig. 1A). p110δ lipid kinase activity was completely abrogated in $p110\delta^{D910A/D910A}$ mice, with no alteration in the kinase activities of p110α and p110β (Fig. 1B). Total class IA PI3K activity was reduced 30 to 50% in thymocytes as well as in mature B and T cells (*13*).

Antibodies to immunoglobulin M and to CD3 (anti-IgM and anti-CD3) were used to stimulate the B and T cell antigen receptors (BcR and TcR), respectively, and phosphorylation of the PI3K target Akt/protein kinase B (PKB) was used as an indirect measure of PI3K activity. In both cases, the induction of phosphoserine-473 [Ser(*P*)^{473}] Akt/PKB was compromised in $p110\delta^{D910A/D910A}$ cells (Fig. 1C). Phosphorylation of the mitogen-activated protein kinase Erk was also reduced in $p110\delta^{D910A/D910A}$ B and T cells (Fig. 1C), which is consistent with the observation that, depending on signal strength, Erk activation can be regulated by PI3Ks (*14*). Ca^{2+} flux in response to anti-IgM crosslinking and to anti-CD3 crosslinking was attenuated in $p110\delta^{D910A/D910A}$ mice (Fig. 1D), in accord with an important role for PI3Ks upstream of Tec family kinase–mediated activation of phospholipase Cγ (PLCγ) and Ca^{2+} signaling by antigen receptors (*3*, *15*). These results implicate p110δ as an important mediator of antigen receptor signals in B and T cells.

The bone marrow of $p110\delta^{D910A/D910A}$ mice had reduced numbers of $B220^+IgM^+$ B cell progenitors (Fig. 2A). More specifically, the ratios of pre- to pro-B cells were altered: in WT mice there were almost four times as many $CD43^-IgM^+$ pre-B cells as $CD43^+IgM^-$ pro-B cells, whereas the $p110\delta^{D910A/D910A}$ mice had equivalent numbers of pre- and pro-B cells (Fig. 2A). The spleens of $p110\delta^{D910A/D910A}$ mice had, on average, 50% fewer cells than the spleens of WT mice, with a more severe reduction of B cells than T cells (*13*). Analysis of the $B220^+$ population in the spleen indicated similar levels of IgM^+IgD^+ follicular B cells; however, the fraction of $CD23^-CD21^+IgM^+$ marginal zone B cells was reduced in $p110\delta^{WT/D910A}$ spleens and was undetectable in the $p110\delta^{D910A/D910A}$ spleens (Fig. 2B). $CD5^+IgM^+$ peritoneal B-1 cells were readily detected in WT mice, were detected to a lesser extent in $p110\delta^{WT/D910A}$ littermates, and were almost undetectable in $p110\delta^{D910A/D910A}$ mice (Fig. 2C). These results show that p110δ plays an important role in the development and differentiation of B cells.

T cell development in the thymus appeared to be normal as judged by CD4 versus CD8 profiles (Fig. 2D). The lymph nodes contained normal ratios of $CD4^+$ and $CD8^+$ T cells, but the expression of CD44, an activation marker that is also used to distinguish $CD44^{lo}$ naïve T cells from $CD44^{hi}$ memory T cells (*16*), was considerably reduced in T cells from $p110\delta^{D910A/D910A}$ mice (Fig. 2E). These results indicate that p110δ plays a role in the differentiation or survival of effector and, possibly, memory T cells. Peripheral blood cell counts appeared normal, with the exception of a twofold increase in the numbers of neutrophils (table S1).

Proliferation of purified B cells by anti-IgM cross-linking was almost completely abrogated (Fig. 3A). In contrast, proliferation in response to anti-CD40, interleukin 4 (IL-4), or lipopolysaccharide (LPS) was impaired but not abrogated (Fig. 3A). Stimulation with anti-CD40 in combination with IL-4 was also impaired (*13*). Proliferation of purified $CD4^+$ T cells in response to anti-CD3 was reduced in $p110\delta^{D910A/D910A}$ mice (Fig. 3B). In contrast, proliferation in response to costimulation with anti-CD3 and anti-CD28 was normal, or even enhanced, in $p110\delta^{D910A/D910A}$ T cells (Fig. 3B). Stimulation of IL-2 production by anti-CD3 and anti-CD28 was normal (Fig. 3C), as was the capacity of phorbol 12,13-dibutyrate (PdBu)–stimulated T cells to proliferate in response to IL-2 (Fig. 3B). To examine the response of T cells to a physiological ligand, we crossed the $p110\delta^{D910A/D910A}$ mice with DO11-10 mice, which express a TcR specific for an ovalbumin peptide [Ova(323–339)] (*17*). T cells from $p110\delta^{D910A/D910A}$ DO11-10 mice exhibited diminished proliferative responses to the Ova peptide presented by WT antigen presenting cells (APCs) (Fig. 3D). IL-2 production was also attenuated in response to peptide stimulation, especially at elevated peptide concentrations (Fig. 3E). These results indicate that p110δ plays an important role in T cell activation but that the requirement for p110δ can be overcome by stimulation through CD28, a receptor that can enhance proliferation and IL-2 production independently of PI3K (*18*). The functional interaction between B and T cells depends on integrins that stabilize cell-cell adhesion. However, anti-CD3–induced cell adhesion to fibronectin via β1 integrins and to ICAM-1 via β2 integrins was unaffected by the $p110\delta^{D910A}$ mutation (Fig. 3F). TcR signaling is thought to be amplified by CD28-dependent accumulation of lipid rafts, membrane structures enriched in signaling proteins, at the interface between the T cell and the APC (*19*). The recruitment of lipid rafts, as induced by

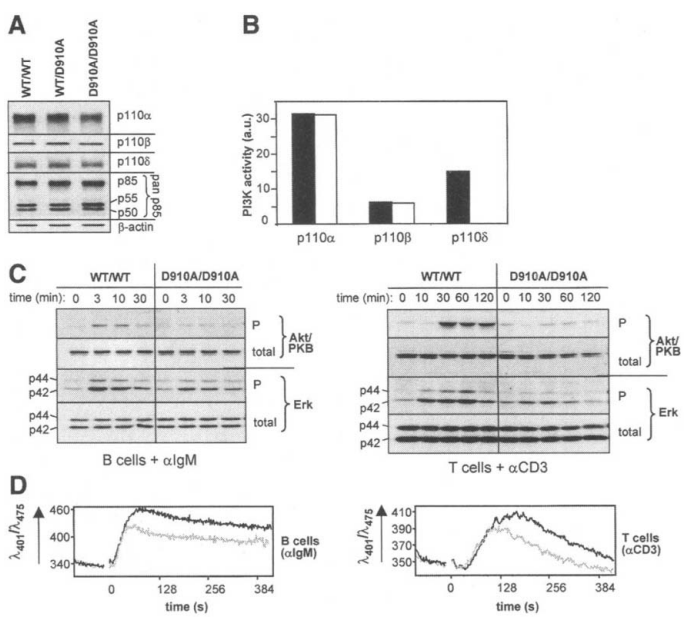

Fig. 1. Impaired PI3K signaling in B and T cells. (**A**) Immunoblots of class IA PI3K subunits expressed in thymocytes. As a control for equal protein loading, the filter was probed with anti-β-actin. (**B**) p110 subunits were immunoprecipitated from thymocyte lysates with isoform-specific antibodies, and the associated lipid kinase activity was assayed with phosphatidylinositol-4,5-bisphosphate as a substrate. Average results from duplicate measurements are represented as arbitrary units (a.u.). No PI3K activity was detected in p110δ immunoprecipitates from $p110\delta^{D910A/D910A}$ mice. Solid bars, WT; open bars, $p110\delta^{D910A/D910A}$. (**C**) Purified B cells were treated with or without soluble anti-IgM (αIgM) $F(ab')_2$ (10 μg/ml). Purified T cells were treated with or without anti-CD3 (αCD3) (10 μg/ml) bound to polystyrene beads. Immunoblots of total cell lysates with antibodies to Akt/PKB [total or Ser(*P*)^{473}] or to Erk [total or Tyr(*P*)^{204}] are shown. (**D**) Ca^{2+} flux was measured in B cells stimulated with αIgM $F(ab')_2$ (10 μg/ml) and in T cells stimulated with αCD3 (5 μg/ml) and anti-hamster immunoglobulin (10 μg/ml) (*24*). Black, WT; gray, $p110\delta^{D910A/D910A}$.

stimulating T cells with beads coated with anti-CD3 and anti-CD28 (*19*, *20*), was about 60% less frequent in p110δ$^{D910A/D910A}$ T cells than in WT T cells (Fig. 3, G and H). Therefore, although raft recruitment appears to be dispensable for T cell activation by antibodies, it may play a critical role during T cell activation by peptide–major histocompatibility complex ligands presented by APCs.

The p110δ$^{D910A/D910A}$ mice had somewhat lower serum immunoglobulin levels than WT littermates, the IgM and IgA isotypes being most consistently reduced (Fig. 4A). To examine in vivo humoral immune responses, we immunized mice with TNP-KLH [(2,4,6-trinitrophenyl)–keyhole limpet hemocyanin] and measured relative TNP-specific antibody titers in the serum on day 12. The total titer of TNP-specific antibodies made by the p110δ$^{D910A/D910A}$ mice was about 4% of that from the WT mice, with a more profound reduction of the IgM, IgG1, and IgG3 isotypes than IgG2a and IgG2b (Fig. 4B). Consistent with these findings, the spleens of TNP-KLH–immunized WT mice contained numerous germinal centers (GCs), whereas formation of these was largely absent in the spleens of TNP-KLH–immunized p110δ$^{D910A/D910A}$ mice (Fig. 4C). These results demonstrate that T cell–dependent humoral immune responses are deficient in p110δ$^{D910A/D910A}$ mice. To measure T cell–independent antibody responses, we immunized mice with TNP-Ficoll and measured relative TNP-specific antibody titers on day 7. Consistent with the impaired capacity of p110δ$^{D910A/D910A}$ B cells to signal through the BcR, T cell–independent humoral responses were strongly impaired (Fig. 4D).

Histological examination revealed lymphoid hypoplasia and lack of GCs in the spleen, lymph nodes, and Peyer's patches (PPs) in p110δ$^{D910A/D910A}$ mice (Fig. 4E, i to iv) (*13*). All other organs appeared to be normal, with the interesting exception of the large intestine. The p110δ$^{D910A/D910A}$ mice developed a mild

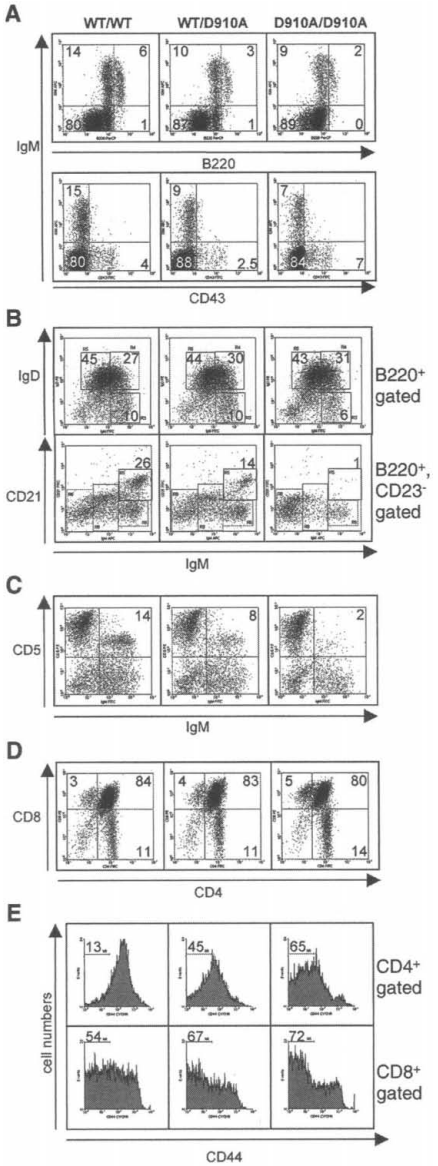

Fig. 2. Impaired B and T cell maturation. Cells from bone marrow (**A**), spleen (**B**), peritoneal washes (**C**), thymus (**D**), and lymph nodes (**E**) were analyzed by flow cytometry with the indicated antibodies (*24*). The percentage of gated cells in particular quadrant is indicated in (A to D). The percentage of CD44^{lo} cells is indicated in (E).

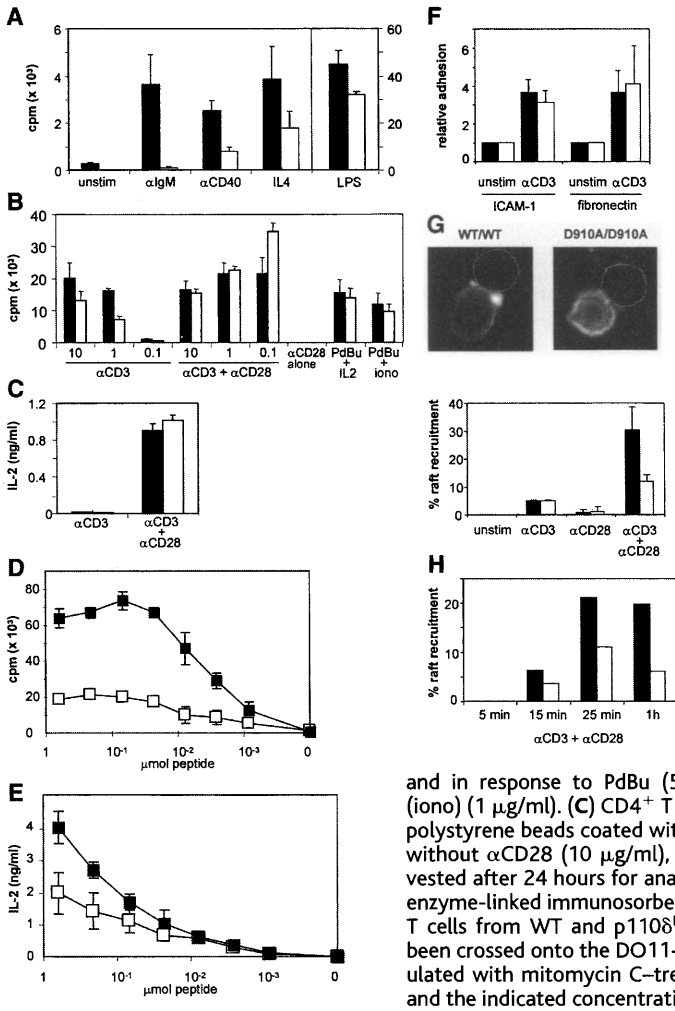

Fig. 3. Impaired B and T cell responses in vitro. (**A**) Purified spleen B cells were stimulated with anti-IgM (αIgM) F(ab')$_2$ (10 μg/ml), αCD40 (10 μg/ml), IL-4 (20 ng/ml), or LPS (10 μg/ml). Proliferation was measured by [^{3}H]thymidine incorporation during the last 6 hours of a 48-hour culture. Similar results were obtained after 24 and 72 hours (*13*). Bars are as in Fig. 1. (**B**) Purified lymph node CD4$^+$ T cells were stimulated with polystyrene beads coated with αCD3 (0.1, 1, or 10 μg/ml) with or without αCD28 (10 μg/ml), and proliferation was measured as described in (A). Proliferation was also measured in response to PdBu (50 ng/ml) and IL-2 (10 ng/ml) and in response to PdBu (50 ng/ml) and ionomycin (iono) (1 μg/ml). (**C**) CD4$^+$ T cells were stimulated with polystyrene beads coated with αCD3 (1 μg/ml) with or without αCD28 (10 μg/ml), and supernatant was harvested after 24 hours for analysis of IL-2 production by enzyme-linked immunosorbent assay (ELISA). (**D**) CD4$^+$ T cells from WT and p110δ$^{D910A/D910A}$ mice that had been crossed onto the DO11-10 background were stimulated with mitomycin C–treated Balb/c spleen B cells and the indicated concentrations of Ova$_{323-339}$ peptide. Proliferation was measured by [^{3}H]thymidine incorporation during the last 6 hours of a 48-hour culture. Solid symbols, WT; open symbols, p110δ$^{D910A/D910A}$ (**E**) CD4$^+$ DO11-10 WT and p110δ$^{D910A/D910A}$ T cells were stimulated as in (D). Supernatants were harvested at 40 hours and assayed for IL-2 content by ELISA. (**F**) Adhesion of T cells stimulated with anti-CD3 to plate-bound fibronectin and ICAM-1 is expressed as fold increase in adhesion of anti-CD3–stimulated versus nonstimulated T cells. (**G**) Purified spleen and lymph node T cells were stimulated for 25 min with polystyrene beads coated with αCD3, αCD28, or αCD3 and αCD28. (Left) Bead (dotted circle) with a WT T cell, scored as positive (presenting raft aggregation toward the bead). (Right) p110δ$^{D910A/D910A}$ T cell/bead complex, scored as negative. Graph represents the percentage of cells presenting raft aggregation toward the bead. The values presented for stimulation by αCD3 and αCD28 are the average of six independent experiments and of two experiments for the other conditions. (**H**) Cells were incubated with αCD3 and αCD28–coated beads, fixed after the indicated incubation times, and analyzed as described in (G). All results presented are from three or four measurements ±SD, except where noted (*24*).

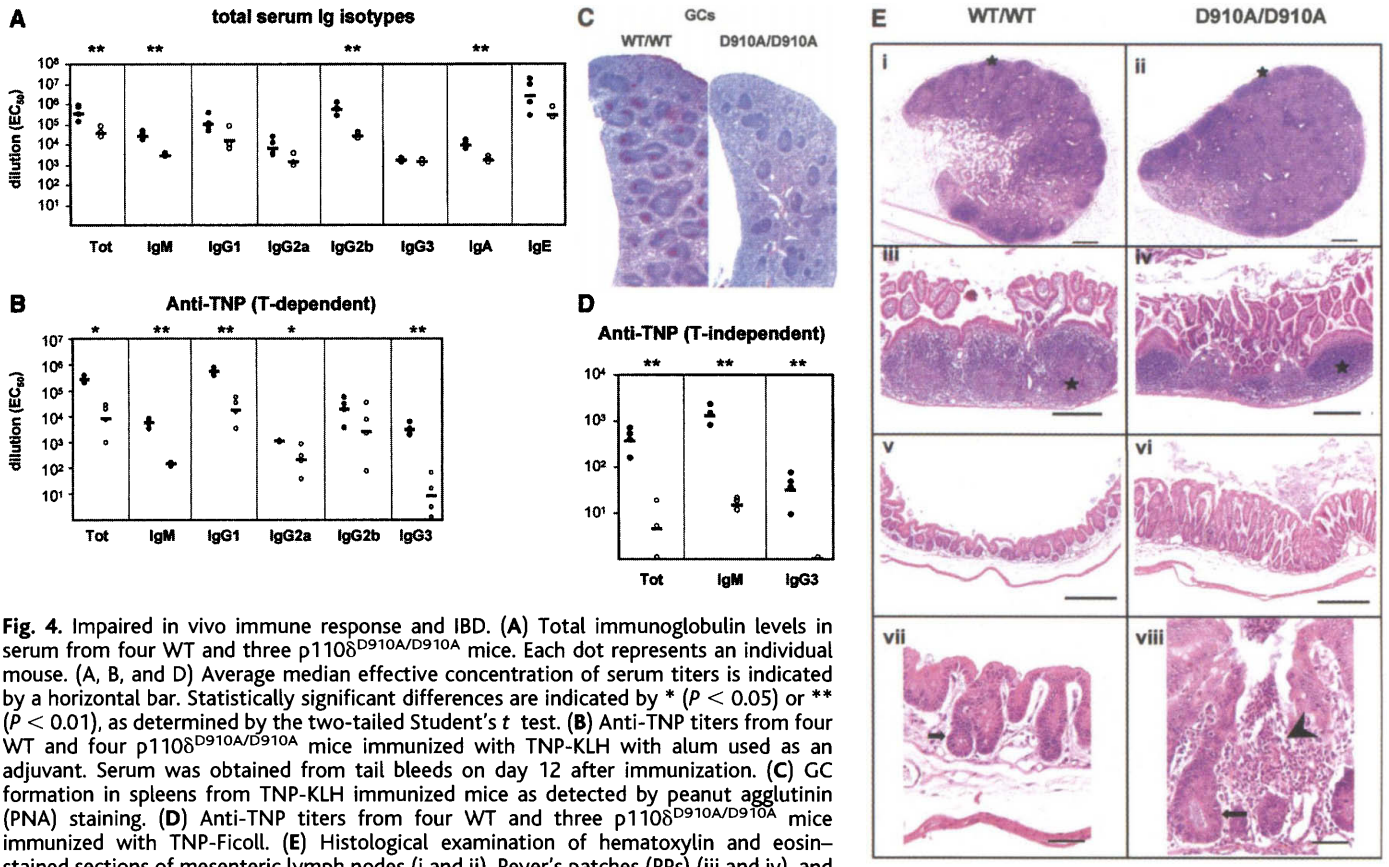

Fig. 4. Impaired in vivo immune response and IBD. (**A**) Total immunoglobulin levels in serum from four WT and three p110δ$^{D910A/D910A}$ mice. Each dot represents an individual mouse. (A, B, and D) Average median effective concentration of serum titers is indicated by a horizontal bar. Statistically significant differences are indicated by * ($P < 0.05$) or ** ($P < 0.01$), as determined by the two-tailed Student's t test. (**B**) Anti-TNP titers from four WT and four p110δ$^{D910A/D910A}$ mice immunized with TNP-KLH with alum used as an adjuvant. Serum was obtained from tail bleeds on day 12 after immunization. (**C**) GC formation in spleens from TNP-KLH immunized mice as detected by peanut agglutinin (PNA) staining. (**D**) Anti-TNP titers from four WT and three p110δ$^{D910A/D910A}$ mice immunized with TNP-Ficoll. (**E**) Histological examination of hematoxylin and eosin–stained sections of mesenteric lymph nodes (i and ii), Peyer's patches (PPs) (iii and iv), and cecum (v to viii) of WT and p110δ$^{D910A/D910A}$ mice. The mesenteric lymph node (i) and the PPs (iii) of WT mice have secondary follicles with prominent GCs (star). GCs are conspicuously absent from the follicles (star) of the mesenteric lymph node (ii) and PPs (iv) of p110δ$^{D910A/D910A}$ mice. (v and vii) Normal intestinal mucosa of the cecum of a control mouse with short crypts (arrow) and sparsely cellular lamina propria. (vi) Cecum of p110δ$^{D910A/D910A}$ mice have thickened mucosa with hyperplasic glands and mixed inflammatory infiltration of the lamina propria. (vii) Higher magnification of the cecum of a p110δ$^{D910A/D910A}$ mouse showing focal erosion of mucosa with neutrophilic inflammation (arrowhead) and a regenerating gland (arrow). (i to vi) Bar, 300 μm; (vii and viii) bar, 50 μm (*24*).

inflammatory bowel disease (IBD), which was segmental and mostly limited to the cecal and rectal sections of the large intestine. The lesions were characterized by mucosal hyperplasia, crypt abscesses, and mixed leukocyte infiltrates, associated with regenerative changes of the glandular epithelium (Fig. 4E, v to viii). Other gene-targeted mice with T cell defects develop IBD, which may reflect an important role for regulatory T cells in maintaining tolerance to gut flora by secreting anti-inflammatory cytokines such as IL-10 and transforming growth factor–β (*21*). IBD in humans, which includes Crohn's disease and ulcerative colitis, can result from inherited mutations in disease susceptibility genes interacting with environmental factors such as the intestinal bacterial flora. The human p110δ gene (*PIK3CD*) maps to the IBD7 susceptibility locus on chromosome 1p36 (*22*, *23*). Given the IBD phenotype of p110δ$^{D910A/D910A}$ mice, *PIK3CD* should be further investigated as a candidate human IBD susceptibility gene.

p110δ plays a unique role in antigen receptor signaling that is not readily compensated for by p110α or p110β. The selective attenuation of immune function in p110δ$^{D910A/D910A}$ mice suggests that a specific inhibitor of p110δ could effectively suppress B and T cell–mediated autoimmunity and possibly B and T cell transformation.

References and Notes

1. B. Vanhaesebroeck *et al.*, *Annu. Rev. Biochem.* **70**, 535 (2001).
2. R. Katso *et al.*, *Annu. Rev. Cell Dev. Biol.* **17**, 615 (2001).
3. D. A. Fruman, L. C. Cantley, *Semin. Immunol.* **14**, 7 (2002).
4. T. Sasaki, A. Suzuki, J. Sasaki, J. M. Penninger, *J. Biochem. (Tokyo)* **131**, 495 (2002).
5. D. A. Fruman *et al.*, *Science* **283**, 393 (1999).
6. H. Suzuki *et al.*, *Science* **283**, 390 (1999).
7. A. Suzuki *et al.*, *Immunity* **14**, 523 (2001).
8. B. Vanhaesebroeck *et al.*, *Proc. Natl. Acad. Sci. U.S.A.* **94**, 4330 (1997).
9. D. Chantry *et al.*, *J. Biol. Chem.* **272**, 19236 (1997).
10. K. Okkenhaug, B. Vanhaesebroeck, *Science's STKE* 16 January 2001. http://stke.sciencemag.org/cgi/content/full/OC_sigtrans;2001/65/pe1
11. J. M. Lu-Kuo, D. A. Fruman, D. M. Joyal, L. C. Cantley, H. R. Katz, *J. Biol. Chem.* **275**, 6022 (2000).
12. L. Bi, I. Okabe, D. J. Bernard, A. Wynshaw-Boris, R. L. Nussbaum, *J. Biol. Chem.* **274**, 10963 (1999).
13. K. Okkenhaug *et al.*, data not shown.
14. B. C. Duckworth, L. C. Cantley, *J. Biol. Chem.* **272**, 27665 (1997).
15. A. M. Scharenberg, J. P. Kinet, *Cell* **94**, 5 (1998).
16. J. Sprent, C. D. Surh, *Annu. Rev. Immunol.* **20**, 551 (2002).
17. K. M. Murphy, A. B. Heimberger, D. Y. Loh, *Science* **250**, 1720 (1990).
18. K. Okkenhaug *et al.*, *Nature Immunol.* **2**, 325 (2001).
19. A. Viola, S. Schroeder, Y. Sakakibara, A. Lanzavecchia, *Science* **283**, 680 (1999).
20. P. J. Ebert, J. F. Baker, J. A. Punt, *J. Immunol.* **165**, 5435 (2000).
21. K. J. Maloy, F. Powrie, *Nature Immunol.* **2**, 816 (2001).
22. N. Seki *et al.*, *DNA Res.* **4**, 355 (1997).
23. J. H. Cho *et al.*, *Hum. Mol. Genet.* **9**, 1425 (2000).
24. Supplementary Methods are available as supporting material on *Science* Online.

25. We thank L. Dobbie, M. Gomez, G. Wame, J. Punt, D. Cantrell, F. Powrie, S. Leevers, D. van Heel, A. Ridley, C. Sawyer, K. Ahmadi, and H. Okkenhaug for help and advice. Supported by the Ludwig Institute for Cancer Research, the UK Biotechnology and Biological Sciences Research Council (B.V., A.J.H.S., and W.P.), Diabetes UK (B.V., A.J.H.S., and A.S.), European Union Fifth Framework Programme QLG1-2001-02171 (B.V. and K.O.), l'Association pour la Recherche sur le Cancer and European Union Marie Curie (G.F.), Fondazione Italiana per la Ricerca sul Cancro and Università di Napoli Federico II (A.B.), and the Flanders Fund for Scientific Research, Belgium (B.V.).

Supporting Online Material

www.sciencemag.org/cgi/content/full/1073560/DC1
Materials and Methods
Fig. S1
Table S1

3 May 2002; accepted 3 July 2002
Published online 18 July 2002;
10.1126/science.1073560
Include this information when citing this paper.